THE JOURNAL OF BIOLOGICAL CHEMISTRY VOL. 287, NO. 23, pp. 19550–19563, June 1, 2012

BLOC-2, AP-3, and AP-1 Proteins Function in Concert with Rab38 and Rab32 Proteins to Mediate Protein Trafficking to Lysosome-related Organelles*[S]

Received for publication, February 9, 2012, and in revised form, April 10, 2012 Published, JBC Papers in Press, April 16, 2012, DOI 10.1074/jbc.M112.351908

Jarred J. Bultema, Andrea L. Ambrosio, Carolyn L. Burek, and Santiago M. Di Pietro[1]

From the Department of Biochemistry and Molecular Biology, Colorado State University, Fort Collins, Colorado 80523

Background: Lysosome-related organelles are a group of cell type-specific compartments with specialized functions, including melanosomes in melanocytes.
Results: Cell type-specific Rab proteins, Rab32 and Rab38, colocalize and interact with the ubiquitous trafficking machinery in melanocytes.
Conclusion: Rab32 and Rab38 cooperate with the ubiquitous trafficking machinery for melanosome biogenesis.
Significance: Learning how lysosome-related organelles are built is key to understanding their biology.

Lysosome-related organelles (LROs) are synthesized in specialized cell types where they largely coexist with conventional lysosomes. Most of the known cellular transport machinery involved in biogenesis are ubiquitously expressed and shared between lysosomes and LROs. Examples of common components are the adaptor protein complex-3 (AP-3) and biogenesis of lysosome-related organelle complex (BLOC)-2. These protein complexes control sorting and transport of newly synthesized integral membrane proteins from early endosomes to both lysosomes and LROs such as the melanosome. However, it is unknown what factors cooperate with the ubiquitous transport machinery to mediate transport to LROs in specialized cells. Focusing on the melanosome, we show that the ubiquitous machinery interacts with cell type-specific Rab proteins, Rab38 and Rab32, to facilitate transport to the maturing organelle. BLOC-2, AP-3, and AP-1 coimmunoprecipitated with Rab38 and Rab32 from MNT-1 melanocytic cell extracts. BLOC-2, AP-3, AP-1, and clathrin partially colocalized with Rab38 and Rab32 by confocal immunofluorescence microscopy in MNT-1 cells. Rab38- and Rab32-deficient MNT-1 cells displayed abnormal trafficking and steady state levels of known cargoes of the BLOC-2, AP-3, and AP-1 pathways, the melanin-synthesizing enzymes tyrosinase and tyrosinase-related protein-1. These observations support the idea that Rab38 and Rab32 are the specific factors that direct the ubiquitous machinery to mediate transport from early endosomes to maturing LROs. Additionally, analysis of tyrosinase-related protein-2 and total melanin production indicates that Rab32 has unique functions that cannot be carried out by Rab38 in melanosome biogenesis.

Lysosome-related organelles (LROs)[2] are a group of cell type-specific membrane-bound compartments with specialized functions (1–4). Examples of LROs include melanosomes, platelet-dense granules, lamellar bodies of lung type II epithelial cells, and lytic granules of cytotoxic T lymphocytes, and natural killer cells. The physiological functions of these organelles are diverse, from the production and storage of melanin pigments (melanosomes) and the regulation of platelet aggregation (dense granules) to killing virus-infected and tumor cells (lytic granules) (1–4). The LROs share common characteristics with lysosomes such as an acidic luminal pH, the presence of lysosome-associated membrane proteins in their limiting membrane, and a common biogenesis pathway (1–4). The close relationship between lysosomes and LROs is further demonstrated by certain human genetic disorders, including the Hermansky-Pudlak syndrome (HPS), that cause abnormalities in both organelle types (2, 4–6).

HPS is a group of autosomal recessive diseases (OMIM 2033000) that are characterized by oculocutaneous albinism (hypopigmentation of eyes and skin) and prolonged bleeding that result from defects in the biogenesis of melanosomes and platelet-dense granules, respectively (2, 4–6). Some HPS patients present additional symptoms due to defects in other LROs, for instance defective lamellar bodies result in fatal pulmonary fibrosis and abnormal lytic granules cause immune deficiency (2, 4–6). In humans, different forms of the disease, named HPS-1 through HPS-9, have been associated with mutations in nine separate genes (2, 4–7). Orthologs of those genes and seven additional genes cause HPS-like disease in 16 mutant mouse strains (4–9). Several of those HPS genes encode proteins that assemble into stable complexes, named adaptor protein complex-3 (AP-3) and biogenesis of lysosome-related organelle complex (BLOC)-1, -2, and -3 (4–10). The function of AP-3 in lysosome biogenesis has been well established; it characterizes a route for trafficking of integral membrane proteins, such as lysosome-associated membrane proteins, from early

* This work was supported, in whole or in part, by National Institutes of Health Grant 1R01HL106186-01A1 (to S. D.P.). This work was also supported by American Heart Association Award 09SDG2280525.
[S] This article contains supplemental Figs. S1–S6.
[1] To whom correspondence should be addressed. Tel.: 970-491-5302; Fax: 970-491-0494; E-mail: santiago.dipietro@colostate.edu.

[2] The abbreviations used are: LRO, lysosome-related organelle; GTPγS, guanosine 5′-3-*O*-(thio)triphosphate; HPS, Hermansky-Pudlak syndrome.

endosome-associated tubules to the limiting membrane of late endosomes and lysosomes (11–13). The melanosome has served as a prototype for LRO biogenesis studies in part because of the availability of both mutant HPS-like mice with obvious coat color phenotype and an excellent cell line model system, the MNT-1 pigmented human melanocytic cells (2, 4–6, 8, 9, 14–16). Analogous to its function in lysosome biogenesis, AP-3 mediates the transport of cargo integral membrane proteins such as the melanogenic enzyme tyrosinase from early endosome-associated tubules to maturing melanosomes (11, 14, 15, 17). In contrast to AP-3, the function of the BLOCs at the molecular level is not well understood. However, BLOC-1 and -2 also localize to early endosome-associated tubules and are part of the machinery that mediates vesicular transport of integral membrane proteins to lysosomes and melanosomes (7, 14, 17–19). Moreover, BLOC-2 defines a trafficking pathway from early endosomes to maturing melanosomes that is parallel to the AP-3-dependent pathway (3, 17). Accordingly, the AP-3 and BLOC-2 single mutant mice are moderately hypopigmented, but the AP-3/BLOC-2 double mutant mice display a severe coat color phenotype (17). Consistently, epistatic defects were observed for the trafficking of a melanosomal cargo protein, tyrosinase-related protein 1 (Tyrp1), in cultured melanocytes isolated from the corresponding single and double mutant mice (17). Other studies have shown alternative routes for tyrosinase exiting early endosome-associated tubules and presumably leading to maturing melanosomes in MNT-1 cells and mouse melanocytes (15). One such route was defined by AP-3 and the other by another member of the AP family, AP-1, which in melanocytes is also involved in a trafficking pathway from early endosomes to melanosomes (15, 20). It has not yet been established if the AP-3-independent pathways originating from early endosome-associated tubules in the different reports (*i.e.* BLOC-2-dependent and AP-1-dependent) correspond to the same or separate trafficking routes (15, 17, 20).

How are LROs formed in relationship with lysosomes? One possibility is that the LRO replaces the lysosome in the specialized cell and that expression of cell type-specific proteins with lysosomal targeting signals provides the organelle with the LRO function in addition to the degradative role of conventional lysosomes. This may be the case for the lytic granule (1). In contrast, most LROs, including melanosomes and platelet-dense granules, coexist with conventional lysosomes as distinct organelles in the same cell (21, 22). Therefore, sorting mechanisms must exist to segregate newly synthesized LRO and conventional lysosomal components (11). This problem is particularly puzzling because most of the known elements of the trafficking machinery such as AP-3 and the BLOCs are shared for the biogenesis of both lysosomes and LROs (1, 3–7, 10, 11, 17). Moreover, these common components of the trafficking machinery are ubiquitously expressed, as expected for a function in lysosome biogenesis (5, 10, 11). Thus, an outstanding question is what are the factors that direct the ubiquitous trafficking machinery toward LROs in cells that simultaneously produce conventional lysosomes (3, 11, 17)?

Rab proteins are GTPases of the Ras superfamily that confer target and timing specificity to vesicle budding, motility, tethering, docking, and fusion within the eukaryotic secretory and endosomal pathways (23, 24). Rab38 and its close homolog Rab32 are expressed in a highly tissue-specific manner, chiefly in LRO-producing cells such as melanocytes, platelets, and lung type II epithelial cells (24–29). Rodent models of HPS with mutations in Rab38 display hypopigmentation, prolonged bleeding, and lung disease due to defective biogenesis of melanosomes, platelet-dense granules, and lamellar bodies, respectively (24–32). The pigmentation phenotype elicited by Rab38 deficiency is mild (25). However, when melanocytes isolated from Rab38 mutant mice were subjected to siRNA knockdown of Rab32, the resulting phenotype was much more severe, and the trafficking of both tyrosinase and Tyrp1 was altered (27). This result placed Rab38 and Rab32 as key players in LRO biogenesis and implied that Rab32 is able to functionally compensate for Rab38, at least in part, or that they operate in parallel pathways (27). This apparently epistatic relationship between Rab38 and Rab32 is analogous to the one described between AP-3 and BLOC-2 and raised the exciting possibility that these Rabs could be the specificity factors that work in concert with the ubiquitous trafficking machinery for transport toward LROs (17, 27). Despite the initial progress made in the field with the discovery of Rab38 and Rab32 involvement in LRO biogenesis, several questions remain unanswered (27, 33). Where do the Rabs function and who are their partners? Can Rab38 functionally compensate for Rab32 deficiency? Do they have nonredundant roles in melanosome biogenesis?

Using gene silencing, biochemical, and imaging approaches, we show that BLOC-2, AP-3, and AP-1 interact physically and functionally with Rab38 and Rab32 to mediate melanosome biogenesis. The results indicate Rab38 and Rab32 operate together with the ubiquitous transport machinery in pathways from early endosomal domains toward maturing melanosomes. Analysis of the three melanin-synthesizing enzymes, tyrosinase, Tyrp1, and Tyrp2, and overall melanin production show Rab38 and Rab32 have both redundant and nonredundant roles in melanosome biogenesis.

EXPERIMENTAL PROCEDURES

Plasmids and Antibodies—The cDNA for Rab32, Rab38, and Rab11 were amplified from total RNAs of MNT-1 cells by reverse transcriptase-PCR and subsequently cloned in-frame into pGEX-5X-1 and pET-30a$^+$ bacterial expression vectors (for expression and purification of GST- and polyhistidine-tagged proteins, respectively). Rabbit and rat polyclonal antibodies were generated against purified GST-Rab38 or GST-Rab32. Antibodies were affinity-purified from sera using either polyhistidine-Rab38 or GST-Rab32 covalently coupled to Affi-Gel 15 beads (Bio-Rad). Anti-Rab32 serum was passed through a GST-Affi-Gel 15 column, to remove anti-GST antibodies.

Other antibodies used are as follows: affinity-purified rabbit antibody to HPS6 (HP6D, gift from E. C. Dell'Angelica (34)); AP-3 β (Protein Tech); mouse monoclonal antibodies against HPS4 and pallidin (gift from E. C. Dell'Angelica (17, 35)); AP-3δ (SA4, gift from A. A. Peden (13)); AP-3μ (18/p47A, BD Biosciences); AP-1γ (100/3, Sigma); clathrin heavy chain (X22, Abcam); Tyrp1 (MEL-5/TA99, Santa Cruz Biotechnology); tyrosinase (T311, Santa Cruz Biotechnology); Tyrp2 (C-9, Santa Cruz Biotechnology); SNX1 (clone 51, BD Biosciences);

EEA1 (clone 14, BD Biosciences); α-tubulin (DM1A, Sigma). Control rabbit IgG was from Southern Biotechnology (Birmingham, AL). Alexa-488- and Alexa-546-conjugated secondary antibodies were from Invitrogen, and horseradish peroxidase (HRP)-conjugated secondary antibodies were from GE Healthcare.

Cell Culture—Human MNT-1 cell line was cultured as described previously (36). Transfection for siRNA was performed using the Nucleofector electroporation system (Lonza) and the NHEM-Neo kit with MNT-1 cells subcultured 2–3 days before transfection. Two sequential siRNAs treatments were performed on days 1 and 4, and cells were analyzed on day 7. Oligonucleotides used for siRNA are as follows: δ subunit of AP-3 (17); HPS6 subunit of BLOC-2 (Sigma, SASI_Hs01_00035287); γ subunit of AP-1 (Sigma, SASI_Hs01_00151148); Rab32 (Sigma, SASI_Hs02_00342400); Rab38 (Sigma, SASI_Hs01_00247037); and HPS4 subunit of BLOC-3 and pallidin subunit of BLOC-1 (17).

Biochemical Procedures—Cytosolic and membrane fractions of MNT-1 cells were prepared by homogenization in buffer A (20 mM HEPES, pH 7.4, 50 mM KCl, 1 mM dithiothreitol, 1 mM EGTA, 1 mM $MgCl_2$, 250 mM sucrose) containing a protease inhibitor mixture (34), followed by centrifugation at 15,000 × *g* for 10 min and then ultracentrifugation at 400,000 × *g* for 15 min, at 4 °C. The final membrane pellet was solubilized in 1 ml of buffer A containing protease inhibitor mixture and 1% (w/v) Triton X-100. Triton X-100 was added to the cytosolic fraction to match the detergent concentration. Both fractions were cleared by centrifugation for 10 min at 15,000 × *g* before immunoprecipitation, which was performed as described above (34) except for the use of buffer A in all washing steps, three times with 0.1% (w/v) Triton X-100, and then once without detergent. Guanidine nucleotide exchange of GST-Rab fusion proteins and GST pulldown assays was performed as described previously (37).

For membrane association experiments, cytosol and membrane fractions were obtained from MNT-1 cells by homogenization in buffer B (10 mM HEPES, pH 7.4, 250 mM sucrose, 1 mM dithiothreitol, 1 mM EGTA, 0.5 mM $MgCl_2$, 0.25 mM GTPγS, and protease inhibitor mixture), followed by centrifugation for 5 min at 15,000 × *g* and for 15 min at 400,000 × *g*, at 4 °C. Immunoblotting was performed as described previously (38).

Quantification of immunoblots was carried out by chemifluorescent detection using a Storm 860 scanner (GE Healthcare) with an excitation wavelength of 450 nm and a 520 LP emission filter or by scanning films. Integration of the band intensities was performed using ImageJ (National Institutes of Health).

Melanin Content—MNT-1 cells were centrifuged at 90 × *g* for 10 min to pellet cells. Cell pellets were treated and analyzed as described previously (39) by a spectrophotometric method at 500 nm using purified *Sepia officinalis* melanin (Sigma) as a standard.

Immunofluorescence Microscopy and Antibody Internalization Assay—Immunofluorescence staining, internalization of antibodies, and leupeptin treatment were performed as described previously (17, 40, 41). Rabbit anti-Rab32 and anti-Rab38 were used in all costaining experiments except for costaining with BLOC-2 (HPS6 subunit) where the corresponding rat anti-Rab32 and anti-Rab38 were utilized. For labeling lysosomes with dextran, cells were incubated for 15 h at 37 °C in medium containing 50 μg/ml of fixable dextran-Alexa Fluor 647 (Invitrogen) followed by a 4-h chase period in medium lacking dextran. Immunofluorescence microscopy samples were examined in a temperature-controlled chamber at room temperature on an Olympus IX81 spinning disc confocal microscope with Photometrics Cascade II camera using a ×100/1.40NA objective. Images were acquired and analyzed in Slidebook version 5 software (3i, Denver. CO). For determination of the percent of colocalization, each channel was subjected to a Laplacian two-dimensional filter with a 3 × 3 kernel (−1, 8, −1), and a binary mask was generated using a Ridler-Calvard automated threshold method both on each channel and on the overlap between the two individual channels in Slidebook software. Pixel area overlap from the overlap mask and each individual mask was used to calculate percent colocalization. Negative controls for colocalization were performed with peroxisomal markers (RFP-SKL and PMP34-GFP, gift from P. K. Kim) that give a similar distributed punctate staining as proteins of interest (42). The degree of colocalization between AP-3, BLOC-2, Rab32, or Rab38 and the peroxisomal markers RFP-SKL and PMP-GFP with this method was below 10%. Antibody internalization images were acquired at room temperature using a Nikon Diaphot 300 microscope with Photometrics Cool SNAP camera using Metamorph software under conditions optimized to prevent signal saturation. Images were analyzed for total fluorescence intensity with ImageJ software as described previously (17).

RESULTS

BLOC-2, AP-3, and AP-1 Interact Physically with Rab38 and Rab32—To study endogenous human Rab38 and Rab32, we raised both rabbit and rat polyclonal antibodies against purified recombinant GST-Rab38 and GST-Rab32 and affinity-purified them as described under "Experimental Procedures". By immunoblotting analysis, both rabbit and rat antibodies to Rab38 recognized the endogenous protein from MNT-1 cell extracts and did not cross-react with Rab32 or any other protein (supplemental Fig. S1). Conversely, both rabbit and rat antibodies to Rab32 recognized the endogenous protein and did not cross-react with Rab38 or any other protein (supplemental Fig. S1). Notice Rab32 has a slightly slower mobility than Rab38, consistent with a 14-residue longer amino acid sequence. Rabbit anti-Rab38 and anti-Rab32 antibodies work very well for immunoprecipitation of the corresponding endogenous protein from MNT-1 cell extracts (supplemental Fig. S1). Immunoprecipitated Rab38 was recognized by both rabbit and rat anti-Rab38 antibodies by immunoblotting, and immunoprecipitated Rab32 was recognized by both rabbit and rat anti-Rab32 antibodies. Importantly, anti-Rab38 antibodies did not immunoprecipitate Rab32, and conversely, anti-Rab32 antibodies did not immunoprecipitate Rab38 (supplemental Fig. S1). As expected, knockdown of Rab38 or Rab32 expression by siRNA treatment of MNT-1 cells resulted in a significant decrease of the corresponding polypeptide, further demonstrating the specificity of the antibodies (supplemental Fig. S2, *lanes 6–8*).

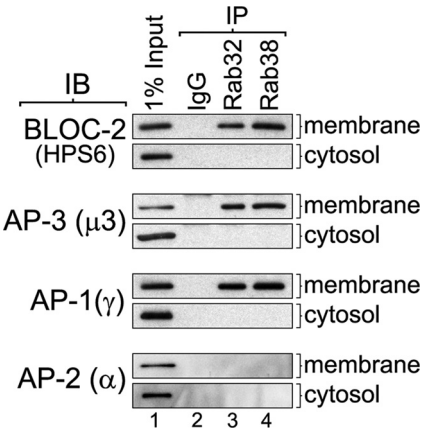

FIGURE 1. **Rab32 and Rab38 coimmunoprecipitate with BLOC-2, AP-3, and AP-1 but not with AP-2.** MNT-1 cells were homogenized in the absence of detergents, and the homogenate was centrifuged to yield cytosolic and membrane fractions. The membrane fraction was solubilized in buffer containing 1% Triton X-100, and the same concentration of detergent was added to the cytosol to match the buffer compositions (see "Experimental Procedures"). Both cytosolic and solubilized membrane fractions were divided into aliquots and subjected to immunoprecipitation (*IP*) using irrelevant IgG, anti-Rab32, or anti-Rab38 rabbit antibodies. The immunoprecipitates, together with an aliquot of the input extracts corresponding to 1% of the material available for immunoprecipitation, were analyzed by immunoblotting (*IB*) using antibodies to the HPS6, μ3, γ, and-α subunits of BLOC-2, AP-3, AP-1, and AP-2, respectively.

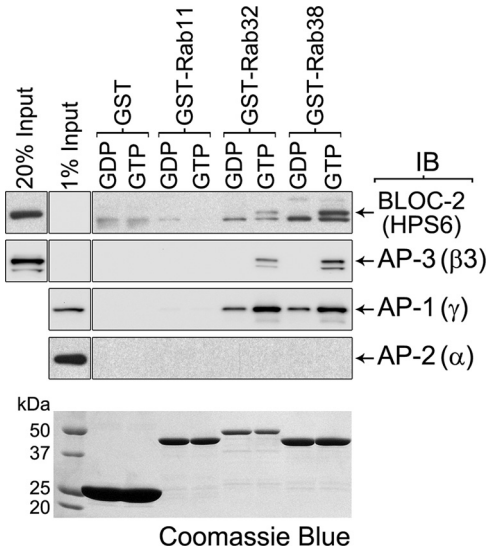

FIGURE 2. **GTP-dependent interaction of Rab32 and Rab38 with BLOC-2, AP-3, and AP-1.** GST pulldown using cytosolic extracts from MNT-1 cells and ~20 μg each of GST, GST-Rab11, GST-Rab32, or GST-Rab38 immobilized on glutathione-Sepharose and loaded with GDP or the stable GTP analog, GTPγS. The washed glutathione-Sepharose beads, together with an aliquot of the input cytosol corresponding to 1 or 20% of the material available for pulldown, were analyzed by immunoblotting (*IB*) using antibodies to the HPS6, β3, γ, and α subunits of BLOC-2, AP-3, AP-1, and AP-2, respectively. The *bottom panel* corresponds to a Coomassie Blue-stained gel and shows the GST fusion proteins.

To test for physical association of Rab38 and Rab32 with BLOC-2, AP-3, and AP-1, MNT-1 cell extracts were subjected to immunoprecipitation under nondenaturing conditions using control IgG, anti-Rab38, or anti-Rab32 antibodies. The washed immunoprecipitates were analyzed by immunoblotting for the presence of BLOC-2, AP-3, and AP-1 using antibodies to the HPS6, μ3, and γ subunits, respectively (Fig. 1). As another specificity control, the immunoprecipitates were also analyzed for the presence of the endocytic adaptor complex AP-2 using antibodies to its α subunit (Fig. 1). BLOC-2, AP-3, AP-1, AP-2, and Rab proteins exist as both soluble and membrane-associated pools (17, 24, 27); therefore, parallel experiments were carried out using both cytosolic and solubilized membrane extracts. As shown in Fig. 1, BLOC-2, AP-3, and AP-1 were detected in the Rab38 and Rab32 immunoprecipitates obtained from solubilized membrane extracts but not from those obtained from cytosolic extracts. Importantly, AP-2 was not detected in the Rab38 or Rab32 immunoprecipitates obtained from solubilized membranes or cytosolic extracts. These results suggest that endogenous Rab38 and Rab32 interact, directly or indirectly, with BLOC-2, AP-3, and AP-1. The finding that it is the membrane-bound form of the Rabs that participates in the interaction suggests a role of the GTP-bound form of the Rabs.

We confirmed the interaction of Rab32 and Rab38 with BLOC-2, AP-3, and AP-1 using pulldown assays. GST-Rab32 and GST-Rab38 were immobilized on glutathione-Sepharose, and their bound nucleotide was exchanged for GDP or GTPγS, a more stable analog of GTP. Subsequently, each Rab was incubated with MNT-1 cytosolic extract, as a source of free BLOC-2, AP-3, and AP-1- supplemented with GDP or GTPγS, respectively. As controls, GST and GST-Rab11 were analyzed in parallel following the same procedure. By immunoblotting we observed that BLOC-2, AP-3, and AP-1 bound to GST-Rab32 and GST-Rab38 but not to GST or GST-Rab11 (Fig. 2). Furthermore, BLOC-2 and AP-3 bound almost exclusively to the GTPγS form of Rab32 and Rab38 compared with the GDP forms (Fig. 2). AP-1 also showed a preference for the GTPγS form of Rab32 and Rab38 but less dramatically than BLOC-2 or AP-3 (Fig. 2). As an additional specificity control, we tested for AP-2, which did not bind to either GST-Rab regardless of the nucleotide form (Fig. 2). These experiments suggest BLOC-2, AP-3, and AP-1 are effectors of Rab32 and Rab38 and that the interactions are likely direct.

BLOC-2 and AP-3 Regulate the Rab38 Association with Membranes—To perform functional studies, we first optimized the conditions to achieve significant knockdown of the targets of interest in MNT-1 cells by siRNA (supplemental Fig. S2). The most efficient gene silencing was obtained using the Nucleofector system for oligonucleotide transfection and subjecting the cells to two sequential siRNA treatments (see "Experimental Procedures" for further details) (43). To address the biological significance of the observed physical interactions of BLOC-2, AP-3, and AP-1 with Rab38 and Rab32, we tested whether membrane association of each Rab was affected by deficiencies in their interacting partners. To this end, cytosolic and membrane fractions were obtained from control MNT-1 cells or cells deficient for BLOC-2, AP-3, or AP-1, and the relative amounts of endogenous Rab38 or Rab32 in the membrane fraction were determined by quantitative immunoblotting (17). About 60% of Rab38 and 95% of Rab32 were found in the membrane fractions of control MNT-1 cells, indicating a stronger Rab32 membrane association at steady state (Fig. 3*A*). Interestingly, the relative amounts of Rab38 recovered from membranes were reduced to about 25% in AP-3-deficient cells and to

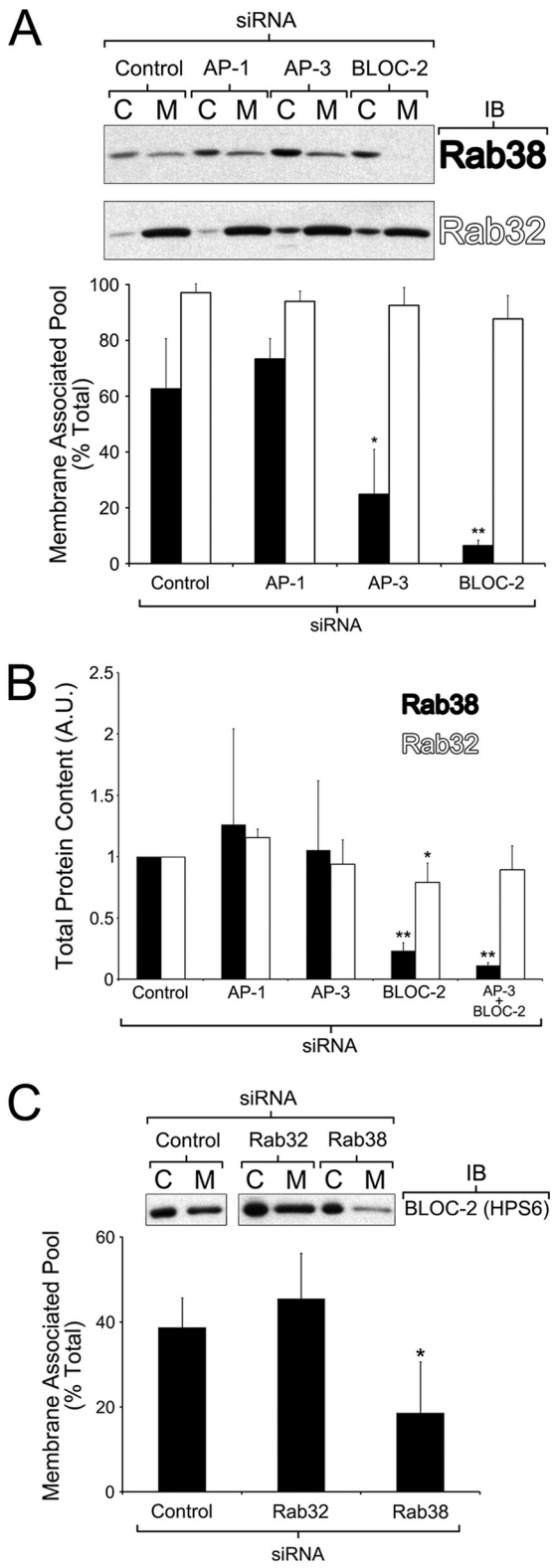

FIGURE 3. **Rab38 association to membranes is altered by AP-3 and BLOC-2 deficiency but only BLOC-2 knockdown affects Rab38 stability.** *A*, MNT-1 cells deficient for AP-1, AP-3, or BLOC-2 together with control cells were subjected to a quick homogenization and ultracentrifugation procedure to yield postnuclear membrane (*M*) and cytosolic (*C*) fractions (see "Experimental Procedures"). The samples were analyzed by immunoblotting (*IB*) using antibodies to Rab32 or Rab38. The *graph* shows the percentage of total Rab38 or Rab32 that was found in the membrane fraction in at least three independent experiments (means ± S.D.). For each Rab protein, the data corresponding to AP-1-, AP-3-, or BLOC-2-deficient cells were compared with that of control cells by means of a *t* test. *B*, quantification of the total amount of Rab32 and Rab38 present in extracts of MNT-1 cells treated with the indicated siRNAs relative to control cells. *Bars* represent means ± S.D. of at least three independent experiments. One sample *t* test was used to compare the results obtained from depleted cells with the reference value of 1 set for control cells. *C*, MNT-1 cells deficient for Rab32 or Rab38 together with control cells were processed as described in *A*. The samples were analyzed by immunoblotting using antibodies to BLOC-2. The *graph* shows the percentage of total BLOC-2 that was found in the membrane fraction in three independent experiments (means ± S.D.). The data corresponding to Rab32- and Rab38-deficient cells was compared with that of control cells by means of a *t* test. *, $p < 0.05$; **, $p < 0.01$.

less than 10% in BLOC-2-deficient cells (Fig. 3*A*). Deficiency of AP-1, however, did not have a statistically significant effect in the fraction of Rab38 recovered from membranes. The relative amount of Rab32 recovered from membranes was somewhat decreased by deficiency in AP-3 or BLOC-2 compared with control cells, but the difference did not reach statistical significance (Fig. 3*A*). Deficiency of AP-1 had no effect on the Rab32 membrane-associated pool. In several replicates of these experiments, the overall amount of Rab38 was noticeably reduced in BLOC-2-deficient cells. Hence, quantitative immunoblotting analysis of the total amount of Rab38 was carried out in extracts from control MNT-1 cells or cells deficient for AP-1, AP-3, BLOC-2, or double deficient for AP-3 and BLOC-2. The total amount of Rab38 was significantly reduced in cells deficient for BLOC-2 or both BLOC-2 and AP-3, but not in AP-1- or AP-3-deficient cells (Fig. 3*B*). A similar analysis for Rab32 showed only a marginal decrease in BLOC-2-deficient cells (Fig. 3*B*). Together, the data suggest that both AP-3 and BLOC-2 regulate or stabilize the Rab38 association with membranes and that BLOC-2 also regulates overall stability of Rab38. The stronger link between Rab38 and BLOC-2 prompted us to examine the converse relationship, *i.e.* if the association of BLOC-2 with membranes was affected by deficiency of Rab38. Indeed, the relative amounts of BLOC-2 recovered from membrane fractions decreased from about 40% in control cells to 20% in Rab38-deficient cells (Fig. 3*C*). In contrast, deficiency of Rab32 did not have any statistically significant effect on the relative amounts of BLOC-2 recovered from membrane fractions (Fig. 3*C*). Overall, the data suggest a stronger connection between Rab38 and the ubiquitous components of trafficking machinery (AP-3 and BLOC-2), compared with Rab32.

BLOC-2, AP-3, and AP-1 Partially Colocalize with Rab38 and Rab32—It is well established that the bulk of both AP-3 and AP-1 localize to clathrin-coated buds on early endosome-associated tubules in MNT-1 and other melanocytic cells (15, 17, 20). This has been shown by immunoelectron microscopy and immunofluorescence microscopy with antibodies to the endogenous complexes (15, 17, 20). Endogenous BLOC-2 was also localized to MNT-1 early endosome-associated tubules by immunoelectron microscopy (17). Given the observed physical association and effect on recruitment to membranes (Figs. 1–3), we sought to determine whether AP-3, AP-1, and BLOC-2 colocalize with Rab38 and Rab32 in MNT-1 cells. Confocal immunofluorescence microcopy was carried out using the same antibodies to AP-3, AP-1, or BLOC-2, as in previous reports (15, 17, 20), and our new antibodies to Rab38 and Rab32 (supplemental Figs. S1 and S2). Analysis of

untreated cell stainings revealed that Rab38 has more cytosolic distribution compared with Rab32 and that Rab32 stains more structures, which is consistent with the biochemical evidence of membrane-associated fractions for these Rabs (Figs. 3*A* and 4 and supplemental Fig. S3). An examination of subcellular distribution of endogenous Rab38 and Rab32 showed that both proteins are mainly found in small puncta in perinuclear and peripheral regions of MNT-1 cells (Fig. 4 and supplemental Fig. S3). Specificity of the staining with Rab38 and Rab32 antibodies was demonstrated by the drastic signal reduction observed upon siRNA knockdown of the corresponding Rab protein (supplemental Fig. S4). A significant degree of colocalization was observed between the adaptor proteins AP-3 (48 ± 2%) or AP-1 (57 ± 2%) and Rab38 in several independent experiments analyzing at least 45 cells (see "Experimental Procedures" for further details) (Fig. 4). There was no discernable difference between AP-3 and AP-1 structures labeled by Rab38 and those without Rab38, and both types of structures are seen throughout the cell. AP-3 and AP-1 also partially colocalized with Rab32 albeit to a lower extent than with Rab38 (35 ± 1 and 37 ± 1%, respectively) (Fig. 4 and supplemental Fig. S3), which suggests that the adaptor proteins may function more closely associated with Rab38 than Rab32. Interestingly, a significant amount of colocalization was observed between clathrin and Rab38 or Rab32 (Fig. 4 and supplemental Fig. S3). Paralleling the relative levels of colocalization with the adaptors, a higher degree of colocalization was observed between clathrin and Rab38 (49 ± 3%) than between clathrin and Rab32 (34 ± 1%). Together, the data indicate Rab38 and Rab32 are likely recruited to early endosomes during the vesicle budding process before the clathrin coat has disassembled. The relative levels of colocalization of AP-3, AP-1, and clathrin with each Rab showed a consistent difference, perhaps indicating Rab38 is recruited earlier than Rab32 during coat formation. In addition, BLOC-2-labeled structures also showed partial colocalization with Rab38 or Rab32 but to a similar extent (Fig. 4 and supplemental Fig. S3). Although the molecular function of BLOC-2 is not clear, it has been suggested to operate both at early endosome-associated tubules and also in downstream transport intermediates (14, 17, 18). It is possible that the Rabs are recruited to nascent vesicles, where they interact with AP-3, AP-1, or BLOC-2, and then remain associated with the vesicles along with BLOC-2.

The above data are compatible with a role of Rab38 and Rab32 in a pathway from specialized early endosome-associated tubules, defined by AP-3, AP-1, and BLOC-2, to maturing melanosomes (Fig. 10). As a control for colocalization between the Rabs and other early endosomal domains, we tested for colocalization with EEA1 and the retromer complex subunit SNX1, which label the vacuolar domain of early endosomes and a retrieval pathway to the *trans*-Golgi network, respectively (Fig. 5). Rab38 showed a very low level of colocalization with EEA1 (4 ± 1%) and SNX1 (4 ± 1%) (Fig. 5) that was comparable with the colocalization of Rab38 and peroxisomal markers used as negative controls and quantified with the same image analysis procedure (see "Experimental Procedures" for further details). Likewise, Rab32 displayed a very low level of colocalization with EEA1 (4 ± 1%) and SNX1 (5 ± 1%) (Fig. 5). We also tested for colocalization between Rab38 and Rab32 with melanosome and lysosome markers. We used Tyrp1 as a well established melanosomal marker that at steady state primarily labels stage III and IV melanosomes and internalized dextran chased for 4 h to label mature lysosomes (Figs. 6 and 10). Both Rab38 and Rab32 showed partial colocalization with Tyrp1 (36 ± 7 and 36 ± 6%, respectively) and negligible colocalization with internalized dextran (1 ± 2 and 2 ± 2%) (Fig. 6).

Melanocytes Deficient for Rab38 and Rab32 Display Abnormal Cargo Trafficking and Steady State Levels—In cells deficient for the ubiquitous components of the trafficking machinery, such as AP-3, AP-1, and BLOC-2, newly synthesized integral membrane protein cargoes are not properly sorted and accumulate in early endosomes. This has been shown both for lysosomal cargo such as LAMP-1 in nonspecialized cells and for melanosomal cargo such as tyrosinase and Tyrp1 in melanocytes (3, 11, 13–15, 17–20, 40, 44). Cargo accumulated in early endosomes can subsequently leak into the recycling pathway to the plasma membrane or enter into the ESCRT-dependent multivesicular body pathway for degradation (Fig. 10) (3, 11, 13–15, 17–20, 40, 44). Therefore, as a consequence of disrupting the normal early endosome to melanosome transport, cargo proteins exhibit increased traffic via the plasma membrane and/or are subjected to degradation (3, 11, 13–15, 17–20, 40, 44). Melanocytes isolated from AP-3- or BLOC-2-deficient mice showed both phenotypes (recycling through the plasma membrane and degradation) when endogenous Tyrp1 was analyzed (17). Melanocytes from AP-3/BLOC-2 double mutant mice showed a more severe defect than each single mutant (17). Here, we sought to determine whether Rab38 and Rab32 deficiency also elicits such phenotypes. Live MNT-1 cells subjected to siRNA treatment targeting each Rab alone or both simultaneously were incubated with antibodies to the luminal domain of Tyrp1 for 20 min and then fixed/permeabilized and processed for fluorescence microscopy. The total fluorescence intensity signal per cell (internalized antibody) was determined for numerous cells per treatment (48–231 cells per treatment), averaged, and normalized to that of control cells (Fig. 7). Deficiency of either Rab38 or Rab32 produces a statistically significant but modest recycling phenotype. Simultaneous deficiency of both Rabs elicits a more pronounced recycling phenotype than either Rab alone. Thus, these results suggest Rab38 and Rab32 are involved in Tyrp1 transport from early endosomes to maturing melanosomes. To compare the relative severity of the Tyrp1 recycling phenotype, similar experiments were carried out in parallel with cells deficient for AP-3 or AP-1 (Fig. 7). The level of Tyrp1 recycling in Rab-deficient cells was comparable with that observed in AP-1-deficient cells but less severe than in AP-3-deficient cells assayed under the same conditions.

A possible caveat with the antibody internalization assay is that the observed surface expression of Tyrp1 could be secondary to increases in total Tyrp1 expression. This possibility was addressed by quantitative Tyrp1 immunoblotting analysis of crude extracts from MNT-1 cells subjected to the corresponding siRNA treatment (Fig. 8*A*). Single Rab38 or Rab32 deficiency caused a marginal decrease in the total levels of Tyrp1, compared with control cells. Deficiency in both Rabs caused a more marked decrease in overall Tyrp1 levels (Fig. 8*A*). There-

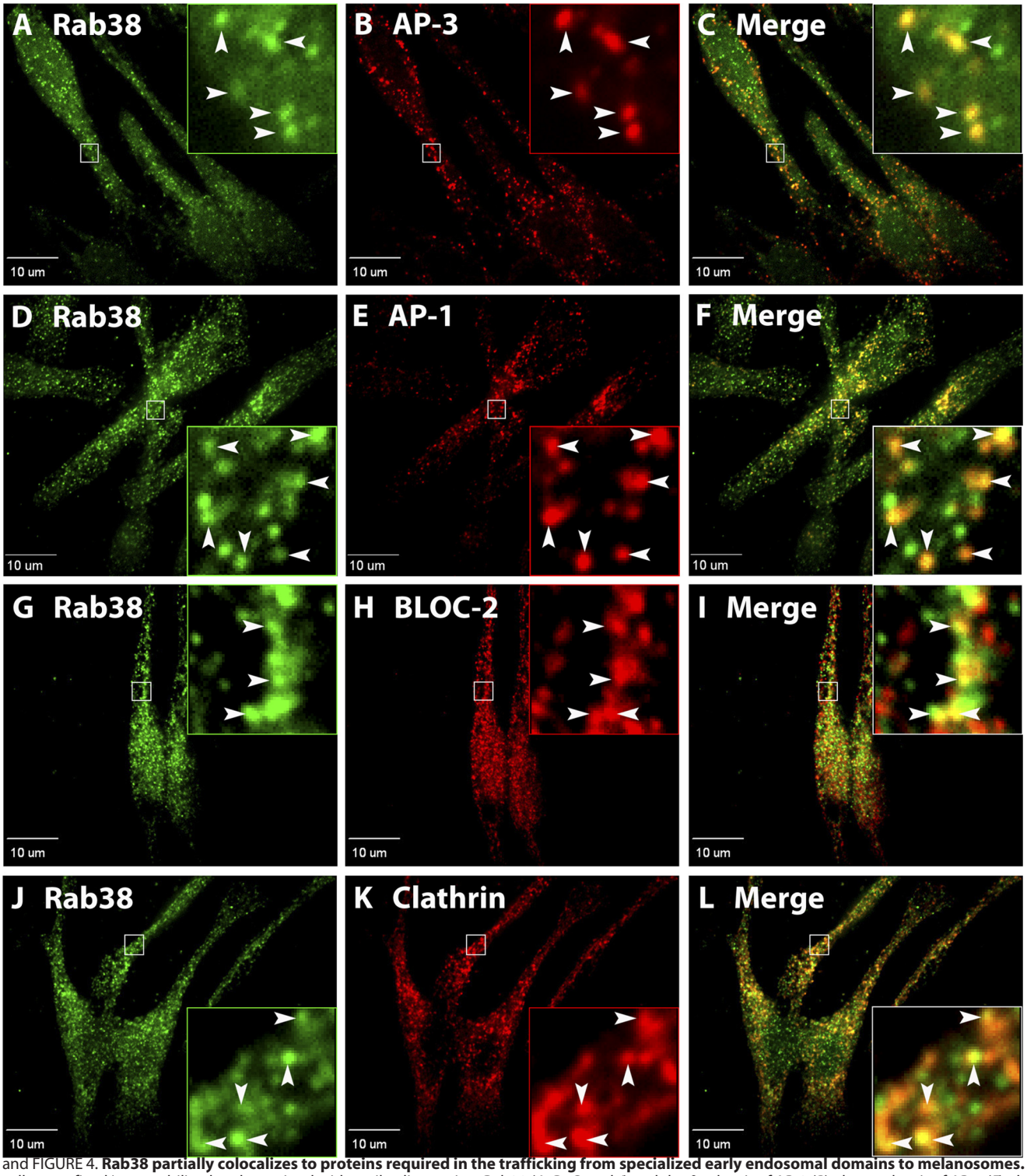

and FIGURE 4. **Rab38 partially colocalizes to proteins required in the trafficking from specialized early endosomal domains to melanosomes.** MNT-1 cells were fixed/permeabilized and costained with antibodies against Rab38 (*A, D, G,* and *J*) and the δ subunit of AP-3 (*B*), the γ subunit of AP-1 (*E*), the HPS6 subunit of BLOC-2 (*H*), or the clathrin heavy chain (*K*). Cells were imaged by confocal fluorescence microscopy, and Rab38 was found both on small structures and in diffuse staining distributed throughout the cells. A significant number of AP-3- (*B*), AP-1- (*E*), BLOC-2- (*H*), and clathrin (*K*)-labeled structures show colocalization with Rab38 in the merged images (*C, F, I,* and *L*). *Boxed areas* are shown in the magnified *insets,* where *arrowheads* indicate sites of colocalization. *Scale bars* indicate 10 μm.

fore, the observed increase in Tyrp1 recycling in Rab -deficient MNT-1 cells is not due to an overall increase in Tyrp1 expression. Moreover, a lower steady state level of Tyrp1 in Rab-deficient cells would be consistent with a scenario in which the melanogenic enzyme cannot properly traffic from early endosomes to maturing melanosomes, thus accumulating in early endosomes and leaking into the degradative multivesicular body pathway (Fig. 10). Following the same approach, extracts from MNT-1 cells deficient for each Rab or both simultaneously were analyzed for the total amounts of tyrosinase and

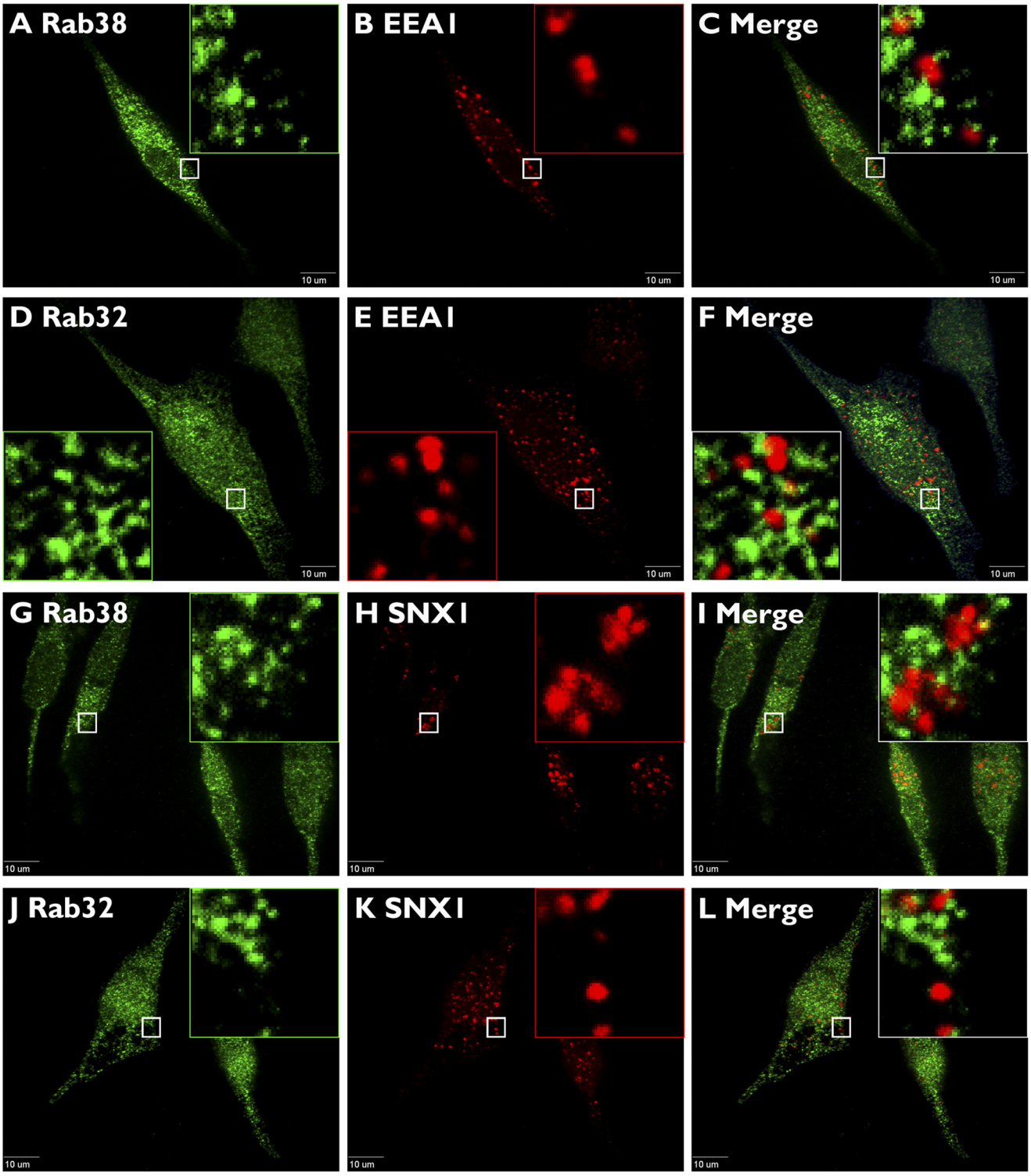

FIGURE 5. **Rab38 and Rab32 do not colocalize to proteins that label early endosome vacuolar domains or the retrieval pathway to the *trans*-Golgi network.** MNT-1 cells were fixed/permeabilized and costained with antibodies against Rab38 (*A* and *G*) or Rab32 (*D* and *J*) and Early Endosome Antigen 1, EEA1 (*B* and *E*), or the retromer subunit Sortin Nexin 1, SNX1 (*H* and *K*). Cells were imaged by confocal fluorescence microscopy, and only background levels of colocalization were detected in the merged images (*C*, *F*, *I*, and *L*). *Boxed areas* are shown in the magnified *insets*. *Scale bars* indicate 10 μm.

Tyrp2, the other two enzymes responsible for melanin synthesis in melanosomes. Tyrosinase was somewhat reduced in Rab38- or Rab32-deficient cells and more so in the double deficient cells, compared with control cells (Fig. 8*A*). Tyrosinase and Tyrp1 followed a similar trend although the defect was more marked for tyrosinase. Notably, Tyrp2 showed a very strong reduction in Rab32-deficient cells but normal levels in Rab38-deficient cells (Fig. 8*A*). The steady state levels of tyrosinase, Tyrp1, and Tyrp2 in single and double Rab-deficient cells were partially rescued by incubation with the lysosomal protease inhibitor leupeptin in agreement with mistrafficking to the degradative pathway in the absence of Rab32/Rab38

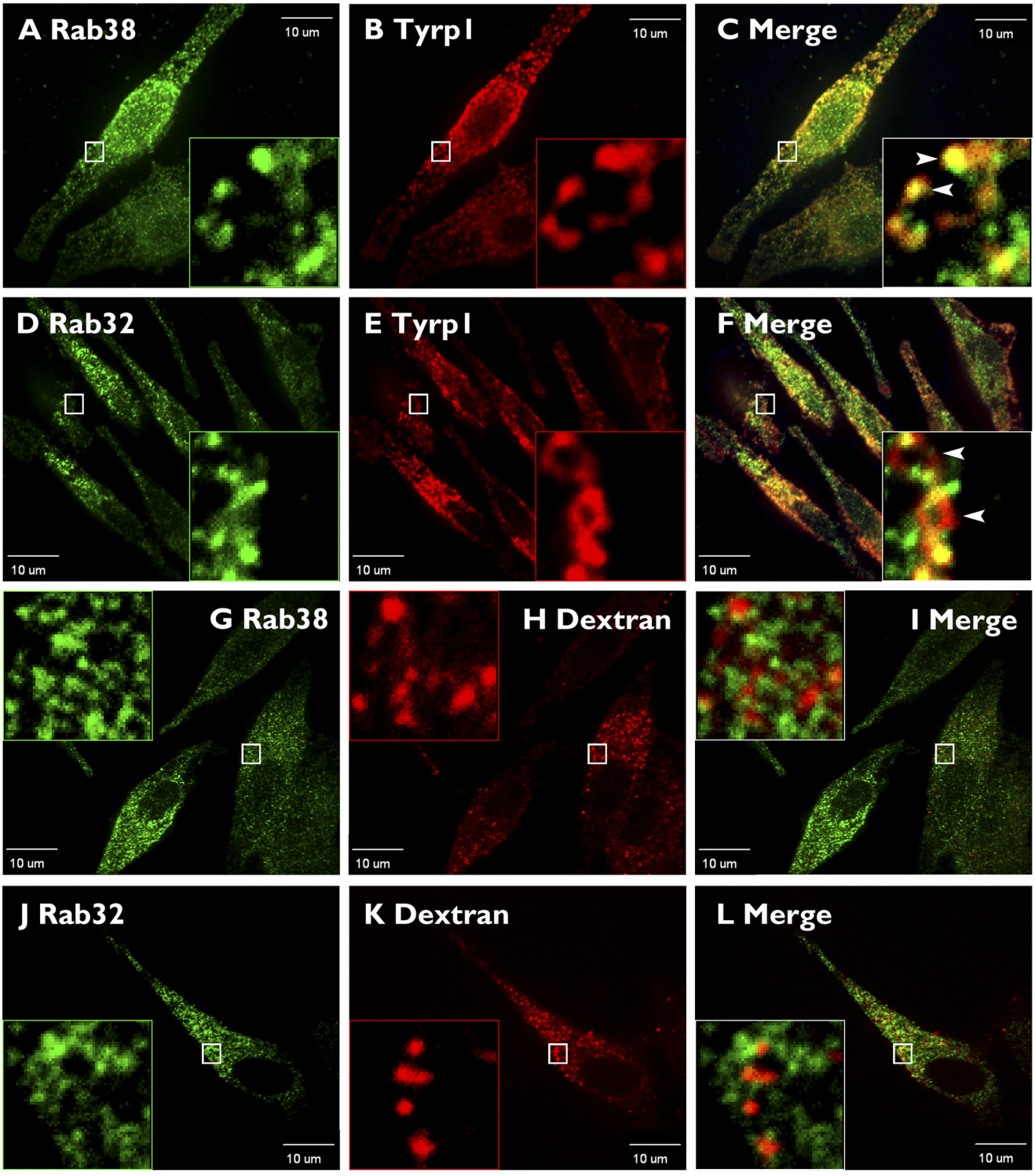

FIGURE 6. **Rab38 and Rab32 partially colocalize to melanosomes but not to lysosomes.** MNT-1 cells were fixed/permeabilized and costained with antibodies against Rab38 (*A*) or Rab32 (*D*) and the melanosomal protein Tyrp1 (*B* and *E*). Alternatively, cells were allowed to internalize dextran/Alexa-647, followed by a chase period of 4 h to ensure specific labeling of mature lysosomes (*H* and *K*), fixed/permeabilized, and stained with antibodies against Rab38 (*G*) or Rab32 (*J*). Cells were imaged by confocal fluorescence microscopy, and both Rab38 and Rab32 were found to partially colocalize with the melanosome marker Tyrp1 (*C* and *F*) but not with lysosomes (*I* and *L*) in the merged images. *Boxed areas* are shown in the magnified *insets*. *Scale bars* indicate 10 μm.

(supplemental Fig. S5). Taken together, these results are consistent with a model in which the Rabs function in the traffic of all three tyrosinase family members from early endosomes to maturing melanosomes. In addition, these results underscore similarities and differences between the Rabs in melanosome biogenesis. On the one hand, both Rabs appear to be involved in the transport of tyrosinase and Tyrp1 in an epistatic fashion such that deficiency in one Rab is not severe because the other Rab can still carry out transport, but deficiency in both Rabs results in a more important phenotype. On the other hand,

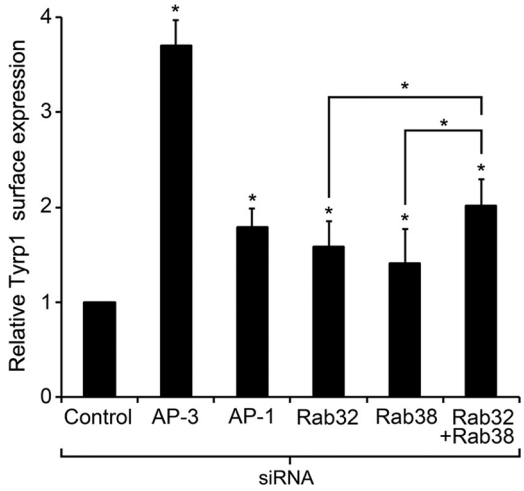

FIGURE 7. **Knockdown of Rab32 or Rab38 causes mistrafficking of Tyrp1.** Live MNT-1 control cells or cells deficient for AP-3, AP-1, Rab32, Rab38, or both Rab32 and Rab38 were incubated in media containing a mouse anti-Tyrp1 antibody for 20 min at 37 °C and subsequently fixed, permeabilized, and immunostained with an Alexa-488-conjugated anti-mouse IgG. Cells were imaged using an epifluorescent microscope, and the relative amounts of internalized anti-Tyrp1 antibody were estimated as the average fluorescence intensity per cell determined with ImageJ and normalized to control cells (means ± S.D.). Result from at least three independent experiments, $n > 48$ for each treatment, were compared with control cells (or between the Rab32/Rab38 double knockdown and the corresponding single knockdowns) by means of a *t* test, *, $p < 0.05$.

Rab32 is strictly necessary to maintain normal Tyrp2 steady state levels, suggesting Rab32 has unique functions in Tyrp2 transport to the maturing melanosome.

Rab32 and Rab38 Functions in Melanosome Biogenesis Are Partially Redundant—Another unresolved matter concerns the relative overall relevance of each Rab for melanosome biogenesis (27, 33). Are they able to functionally compensate for each other? The fact that the Rab38 mutant mouse, *chocolate*, is hypopigmented indicates that Rab32 cannot fully compensate for Rab38 deficiency (25). Is the converse also true? Analysis of the cargo enzymes suggests partial functional compensation between the Rabs for tyrosinase and Tyrp1 traffic to maturing melanosomes, but Rab32 appears to be strictly necessary for normal Tyrp2 traffic (Figs. 7 and 8*A*). Analysis of particular cargo proteins gives important clues but also has its limitations, and we do not yet know the identity or roles of all the cargo proteins involved in melanosome formation (45). Therefore, overall melanin production is probably the most faithful and quantitative measure of proper melanosome biogenesis and an adequate way to determine to what extent a particular component is needed (9, 17, 20, 46). By visual inspection, we consistently noticed that Rab32-deficient MNT-1 cells were significantly hypopigmented, even more so than cells deficient for Rab38. This was particularly apparent after collecting the cells by centrifugation. To test whether the observed differences were significant, total melanin was extracted and quantified from MNT-1 control cells or cells deficient for Rab38 and Rab32 or simultaneously both Rab38 and Rab32. Several independent replicates were carried out, and AP-1-deficient cells were also analyzed for comparison. Consistent with the mild hypopigmentation of *chocolate* mice, Rab38 deficiency caused a moderate loss of melanin in MNT-1 cells (Fig. 8*B*). Importantly,

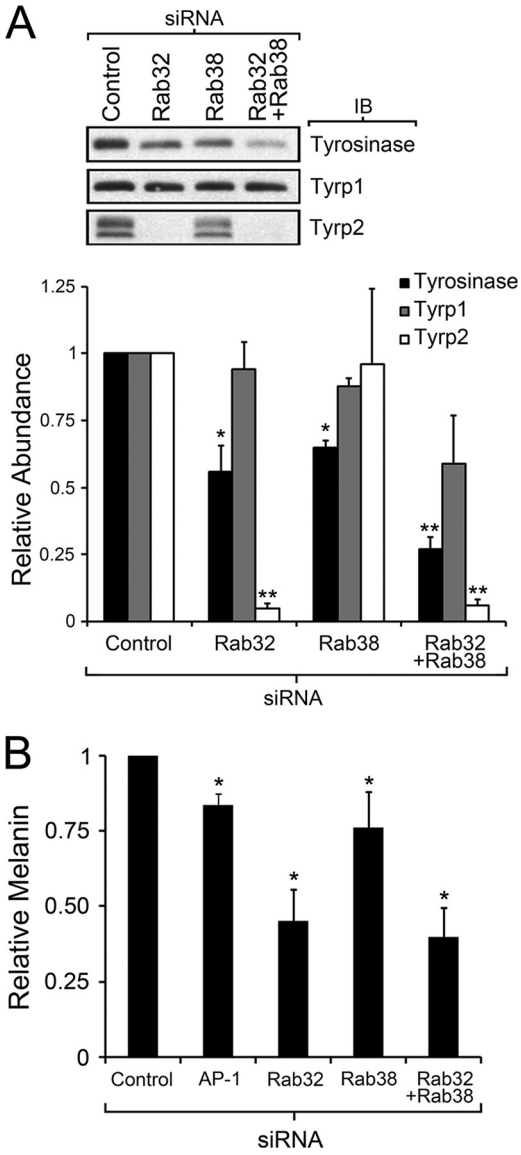

FIGURE 8. **Rab32 and Rab38 are required for normal steady state levels of tyrosinase, Tyrp1, and Tyrp2 and are not fully redundant in overall melanosome biogenesis.** *A*, immunoblotting analysis of total cell extracts from control MNT-1 cells and cells deficient for Rab32, Rab38, or both Rab32 and Rab38 was performed and quantified to determine the total abundance of tyrosinase (*black*), Tyrp1 (*gray*), and Tyrp2 (*white*) relative to control cells. Results correspond to three independent experiments normalized to number of cells, and compared using the *t* test, *, $p < 0.05$; **, $p < 0.01$. *B*, melanin was extracted from MNT-1 control cells or cells deficient for AP-1, Rab32, Rab38, or both Rab32 and Rab38 and quantified by a spectrophotometric method. Results correspond to at least three independent experiments normalized to number of cells and abundance of melanin in control cells, *, $p < 0.05$.

Rab32-deficient MNT-1 cells contained less melanin than control cells (and Rab38- or AP-1-deficient cells) (Fig. 8*B*). This result suggests Rab32 is a critical component for mature melanosome biogenesis and that Rab38 cannot fully compensate for Rab32 deficiency. Consistent with a significant role for Rab32 in overall melanosome biogenesis, Rab32/Rab38 double deficiency did not significantly worsen the phenotype elicited by Rab32 single deficiency (Fig. 8*B*). One trivial explanation for these results is that MNT-1 cells may express substantially more Rab32 than Rab38, but we found comparable amounts of both Rabs by quantitative immunoblotting of total cell extracts.

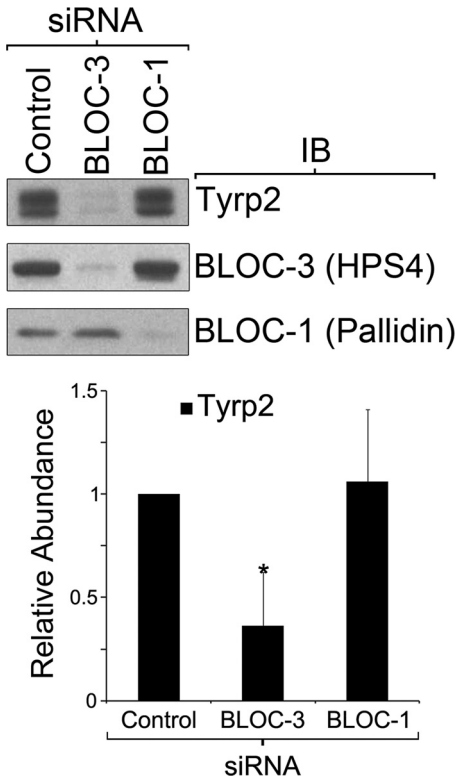

FIGURE 9. **Cells deficient for BLOC-3 display abnormal Tyrp2 steady state levels.** Immunoblotting (*IB*) analysis of total cell extracts from control MNT-1 cells and cells deficient for BLOC-3 or BLOC-1 was performed and quantified to determine the total abundance of Tyrp2 relative to control cells. Results correspond to three independent experiments normalized to number of cells and compared using the *t* test, *, $p < 0.05$.

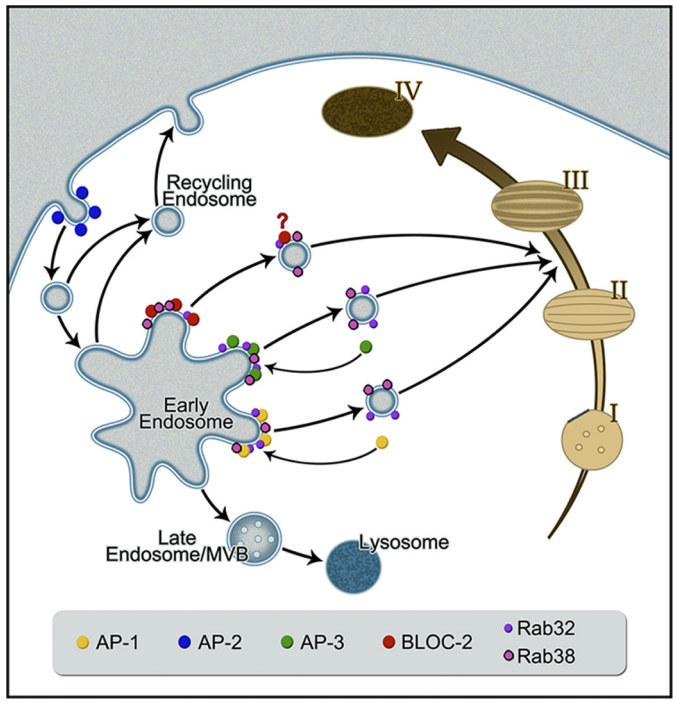

FIGURE 10. **Model for AP-3, AP-1, and BLOC-2 cooperation with Rab38 and Rab32 to mediate transport to maturing melanosomes.** Rab38 and Rab32 interact with AP-3, AP-1, and BLOC-2 at early endosome membrane domains where cargo such as the tyrosinases are concentrated and packaged into transport intermediates. Upon budding, some components of the coat (AP-3, AP-1, and clathrin) dissociate from the vesicle but others remain bound (Rab32, Rab38, and possibly BLOC-2) to mediate further transport, tethering, and fusion with maturing melanosomes. During melanosome biogenesis, transition between stage II and stage III occurs upon incorporation of the melanogenic enzymes with the concomitant beginning of melanin synthesis, and thus vesicles defined by Rab32 and Rab38 likely target this melanosome maturation stage. Deficiency in different components of these pathways elicits cargo accumulation in the early endosomes that eventually leaks into other pathways such as the recycling pathway toward the plasma membrane or the late endosome/multivesicular body (*MVB*) degradative pathway.

In fact, Rab38 is expressed at slightly higher rather than lower levels compared with Rab32 (130 *versus* 89 pg of Rab per μg of total proteins) (supplemental Fig. S6). Additionally, no compensatory up-regulation of Rab32 was observed upon siRNA knockdown of Rab38 or vice versa (supplemental Fig. S2). Taken together, these results imply that the Rabs cannot fully functionally compensate for each other during biogenesis of mature melanosomes.

Melanocytes Deficient for BLOC-3 but Not BLOC-1 Display Abnormal Tyrp2 Steady State Levels—To test the possibility that Tyrp2 transport depends on BLOC-1 or BLOC-3, we carried out quantitative Tyrp2 immunoblotting analysis of crude extracts from MNT-1 cells subjected to the corresponding siRNA treatment (Fig. 9). MNT1 cells deficient for BLOC-3 displayed a statistically significant decrease in Tyrp2 steady state levels, whereas BLOC-1 deficiency had no effect (Fig. 9).

DISCUSSION

The finding that cell type-specific Rab38 and Rab32 are involved in the biogenesis of LROs raised the possibility that these proteins could operate together with the ubiquitous trafficking machinery for transport toward LROs in specialized cell types (24–31). However, no evidence has been reported for a link between the BLOC or AP complexes involved in LRO biogenesis and Rab38 or Rab32. In this study, we demonstrate that AP-3, AP-1, and BLOC-2 interact physically and functionally with Rab38 and Rab32 to mediate transport of integral membrane proteins from specialized early endosomal domains to maturing melanosomes.

We show that endogenous Rab38 and Rab32 can associate with AP-3, AP-1, and BLOC-2 into macromolecular assemblies that are stable enough to allow detection by coimmunoprecipitation (Fig. 1). Our results show the interactions between the Rabs and AP-3, AP-1, and BLOC-2 occur on membranes but not in the cytosol, suggesting a role of the GTP-bound form of the Rabs. Indeed, in GST-Rab pulldown experiments, the interactions showed a strong preference for the GTP form of the Rabs. Because cytosolic AP-3, AP-1, and BLOC-2 presumably represent the "free form" of these complexes, their interaction with purified GST-Rab38 and GST-Rab32 are likely direct, although the possibility of a bridging protein cannot be ruled out. Consistent with these physical interactions, a significant degree of colocalization was observed between AP-3, AP-1, and BLOC-2 and the Rabs (Fig. 4 and supplemental Fig. S3). The bulk of AP-3 and AP-1 has been shown to localize to coated structures budding off from distinct tubular early endosomes or vesicles in MNT-1 and other melanocytic cells (Fig. 10) (15, 17, 20). In line with these observations, clathrin partially colocalized with the Rabs, but markers of other endosomal domains, EEA1 and the retromer complex, did not. Moreover, clathrin

partially colocalized with Rab38 and Rab32 to a similar degree as the clathrin adaptors AP-3 and AP-1, suggesting that the Rabs are recruited in the budding process.

In support of the idea that the interactions of AP-3, AP-1, and BLOC-2 with the Rabs are biologically relevant, we show that knockdown of either Rab38 or Rab32 or both simultaneously elicits the same phenotypes as deficiency in AP-3, AP-1, or BLOC-2. On the one hand, deficiency in the Rabs causes enhanced Tyrp1 recycling through the plasma membrane, a defect previously observed in primary melanocytes from AP-3 and BLOC-2 mutant mice and also detected here in MNT-1 cells deficient for AP-3 or AP-1 (Fig. 7) (17). On the other hand, Rab deficiency elicits reduced overall levels of the tyrosinase family members paralleling the results obtained with melanocytes from AP-3 and BLOC-2 mutant mice, or from HPS patients with mutations in AP-3 and BLOC-2 (Fig. 8*A*) (17, 47, 48). These cargo trafficking data, together with the physical interactions and colocalization results, are most consistent with a model in which the Rabs function in pathways from early endosome-associated tubules to maturing melanosomes (Fig. 10). Such a location fits well with the established model for AP-3-, AP-1-, and BLOC-2-dependent transport of tyrosinase and Tyrp1 from early endosomes to maturing melanosomes and places the Rabs as acting downstream of the early endosome with potential roles in vesicle motility or fusion events (3, 14, 15, 17, 18, 20, 44). This model also provides a satisfactory explanation to the observed cargo phenotypes. Disruption of transport from early endosomes toward melanosomes causes accumulation of the cargo in early endosomes and leakage into the recycling pathway to the plasma membrane and/or into the degradative multivesicular body/lysosomal pathway. This model is also compatible with a previous electron microscopy study that found overexpressed GFP-Rab38 in both MNT-1 cells and mouse melanocytes localized to tubules, vesicles, and melanosomes (27). These three structures (tubules, vesicles, and melanosomes) contained tyrosinase and Tyrp1 and would correspond to the model donor compartment, transport intermediate, and target organelle, respectively (Fig. 10). In fact we also found that both endogenous Rab38 and Rab32 partially colocalize with melanosomes, thus supporting the proposed model (Figs. 6 and 10). Finally, this model is consistent with the recently discovered interaction between the Rab38/32 effector protein Varp and VAMP7 (46, 49). Varp plays a role in Tyrp1 transport to the melanosome, and VAMP7 is a well known vesicle SNARE protein of the AP-3- and BLOC-1-dependent pathway involved in vesicle fusion with late endosomes/lysosomes (11, 19). Alternatively or in parallel, Rab32 and Rab38 might participate in a post-Golgi route that goes from the *trans*-Golgi network directly to the maturing melanosomes, without an early endosome step between the *trans*-Golgi network and melanosomes (27). For all the reasons discussed above, we favor the early endosome route as the main Rab32/Rab38-dependent pathway to maturing melanosomes.

The Tyrp1 recycling phenotype found in AP-3-depleted MNT-1 cells (Fig. 7) recapitulates a similar observation made with melanocytes from AP-3 mutant mice using the same approach (17). This result seems to be at variance with that of a previous article reporting a relatively normal steady state localization of Tyrp1 in fixed melanocytes from patients with AP-3 deficiency (48). However, we note that the Tyrp1 immunofluorescence staining shown in that report in AP-3-deficient melanocytes appears to be significantly less intense than in normal melanocytes (48), thus in agreement with our previous results with melanocytes from AP-3 mutant mice (17) and results presented here with MNT-1 cells. It is likely that in AP-3-deficient cells, a proportion of Tyrp1 molecules eventually reach the melanosomes using the AP-1/BLOC-2 route(s) thus explaining the fixed cell analysis in the earlier report (48). The recycling assay with live cells is designed to detect molecules transiently exposed at the cell surface with high sensitivity that would be difficult to appreciate at steady state by confocal fluorescence or thin section electron microscopy. A complete understanding of the adaptor requirement for transport of each tyrosinase family member will require further elucidation.

Results presented here shed light on aspects of Rab38 and Rab32 that were previously unexplored (33). Our findings suggest Rab38 and Rab32 have functional similarities and differences in melanosome biogenesis. For instance, both Rabs interact with AP-3, AP-1, and BLOC-2; however, the connection with Rab38 is stronger than with Rab32, and our data suggest it is possible that Rab38 operates earlier than Rab32 in the pathways from early endosomes to maturing melanosomes. First, AP-3, AP-1, and clathrin display a higher degree of colocalization with Rab38 than with Rab32 (Fig. 4 and supplemental Fig. S3). Second, Rab38 association with membranes is decreased after knockdown of AP-3 or BLOC-2 but Rab32 is only marginally affected (Fig. 3*A*). The functional relationship between Rab38 and BLOC-2 is particularly strong. BLOC-2 deficiency affected most severely the Rab38 association with membranes and also compromised the overall Rab38 stability (Fig. 3, *A* and *B*). Conversely, Rab38 (but not Rab32) deficiency affected BLOC-2 association with membranes (Fig. 3*C*). This level of interdependence between BLOC-2 and Rab38 resembles the one observed between subunits of the same BLOC or AP complex (10, 40). For instance absence of a BLOC-2 subunit such as HPS3 causes a destabilization (although not complete absence) of the other two subunits (HPS5 and HPS6) (50). Further confirming the strong Rab38-BLOC-2 connection, the coat color of the chocolate mouse (with a Rab38 mutation) is very similar to the BLOC-2 mutant strains, cocoa (HPS3), ruby-eye (HPS6), and ruby-eye-2 (HPS5) (25, 29, 50). Nevertheless, the Rab38 association with BLOC-2 is likely transient rather than as components of a stable complex. Unlike AP-3 and AP-1, the molecular function of BLOC-2 is unknown. The tight association with Rab38 discovered here will help future elucidation of BLOC-2 function at the molecular level.

Our results show additional similarities and differences between Rab38 and Rab32 in terms of their requirement for trafficking of specific cargoes and overall relevance for melanosome biogenesis. Single deficiency in each Rab causes similar and relatively modest Tyrp1 recycling phenotype or decrease in the steady state levels of tyrosinase and Tyrp1 (Figs. 7 and 8*A*). In contrast, we observed drastically different effects for Tyrp2 steady state levels, which were severely reduced in Rab32-deficient cells but not affected in Rab38-deficient cells. In addition, tyrosinase and Tyrp1 trafficking phenotypes are more severe in

cells simultaneously deficient for both Rabs, compared with single deficient cells (Figs. 7 and 8*A*). Thus, Rab32 appears to more clearly cooperate with Rab38 in pathways utilized by cargo such as tyrosinase and Tyrp1, which are also known to depend on AP-3, AP-1, and BLOC-2 (4, 11, 14, 15, 17, 18, 20, 47, 48, 51). Interestingly, the trafficking of Tyrp2 has been far less characterized compared with that of tyrosinase and Tyrp1. Our data suggest that Tyrp2 utilizes a pathway in which Rab32 is strictly necessary and that it is at least partially different from those of tyrosinase and Tyrp1 (Fig. 8*A*). This result is consistent with the finding that Tyrp1 but not Tyrp2 associates with tyrosinase in murine melanocytes *in vivo* (52). This apparently Rab38-independent pathway toward melanosomes utilized by Tyrp2, and perhaps other melanosome components, would provide an explanation for the incomplete compensation by Rab38 in Rab32-deficient cells as assessed by melanin content (Fig. 8*B*). Conversely, incomplete compensation by Rab32 in Rab38-deficient MNT-1 cells (Fig. 8*B*) is consistent with the pigmentation defect of the *chocolate* mouse (25). Therefore, the emerging picture is one in which the Rabs are only partially redundant for melanosome biogenesis.

An interesting question is how does Rab32 carry out its unique non-Rab38 redundant functions in melanosome biogenesis such as Tyrp2 traffic? As stated above, this trafficking route appears to be different from the routes used by tyrosinase and Tyrp1, which are also known to depend on AP-3, AP-1, and BLOC-2 (4, 11, 14, 15, 17, 18, 20, 47, 48, 51). It is possible that such a Tyrp2/Rab32 route is dependent on other components of the ubiquitous machinery involved in melanosome biogenesis, such as BLOC-1 or BLOC-3. Analysis of MNT1 cells deficient for BLOC-3 showed significantly decreased steady state levels of Tyrp2, although BLOC-1 deficiency had no effect (Fig. 9). The Tyrp2 phenotype caused by BLOC-3 deficiency resembles that elicited by Rab32 deficiency (Fig. 8*A*). This result raises the possibility that Rab32 participates in a separate route to melanosomes that is dependent on BLOC-3 and used by cargo such as Tyrp2. The molecular function of BLOC-3 is unknown. Our results suggest a framework for the Rab32 unique functions (nonredundant with Rab38) and will be important for future studies aimed at elucidating the function of BLOC-3. Rab32 may have additional unique functions unrelated to LRO biogenesis as it was also reported to modulate the mitochondrially associated membrane properties (53).

In conclusion, our results point to a novel mechanism for directing the ubiquitous trafficking machinery from early endosomes toward maturing melanosomes and likely other LROs. Tissue-specific Rab proteins, Rab38 and Rab32, interact with AP-3, AP-1, and BLOC-2 and likely identify specialized early endosomal domains for budding of transport intermediates destined for maturing melanosomes. It is possible that a ubiquitous Rab could define analogous early endosomal domains for transport of membrane proteins to conventional lysosomes. This could be the function of Rab7, which is involved in transport to lysosomes and has recently been shown to be co-recruited with AP-3 to artificial membranes containing the endosomal phospholipid phosphatidylinositol-3 phosphate (54). We also obtained evidence that the Rabs have both overlapping and exclusive functions for overall melanosome biogenesis and traffic of specific cargoes. Further study is needed to dissect the mechanisms by which Rab38 and Rab32 execute redundant and unique functions in trafficking to LROs.

Acknowledgments—We thank Andrew A. Peden, Esteban C. Dell'Angelica, and Peter K. Kim for their generous gifts of reagents and Vincent J. Hearing for guidance with the Nucleofector system for MNT-1 transfection. Microscopes used in this work are supported in part by the Microscope Imaging Network core infrastructure grant from Colorado State University.

REFERENCES

1. Dell'Angelica, E. C., Mullins, C., Caplan, S., and Bonifacino, J. S. (2000) Lysosome-related organelles. *FASEB J.* **14,** 1265–1278
2. Spritz, R. A., Chiang, P. W., Oiso, N., and Alkhateeb, A. (2003) Human and mouse disorders of pigmentation. *Curr. Opin. Genet. Dev.* **13,** 284–289
3. Raposo, G., Marks, M. S., and Cutler, D. F. (2007) Lysosome-related organelles. Driving post-Golgi compartments into specialization. *Curr. Opin. Cell Biol.* **19,** 394–401
4. Huizing, M., Helip-Wooley, A., Westbroek, W., Gunay-Aygun, M., and Gahl, W. A. (2008) Disorders of lysosome-related organelle biogenesis. Clinical and molecular genetics. *Annu. Rev. Genomics Hum. Genet.* **9,** 359–386
5. Di Pietro, S. M., and Dell'Angelica, E. C. (2005) The cell biology of Hermansky-Pudlak syndrome. Recent advances. *Traffic* **6,** 525–533
6. Wei, M. L. (2006) Hermansky-Pudlak syndrome. A disease of protein trafficking and organelle function. *Pigment Cell Res.* **19,** 19–42
7. Cullinane, A. R., Curry, J. A., Carmona-Rivera, C., Summers, C. G., Ciccone, C., Cardillo, N. D., Dorward, H., Hess, R. A., White, J. G., Adams, D., Huizing, M., and Gahl, W. A. (2011) A BLOC-1 mutation screen reveals that PLDN is mutated in Hermansky-Pudlak syndrome type 9. *Am. J. Hum. Genet.* **88,** 778–787
8. Li, W., Rusiniak, M. E., Chintala, S., Gautam, R., Novak, E. K., and Swank, R. T. (2004) Murine Hermansky-Pudlak syndrome genes. Regulators of lysosome-related organelles. *BioEssays* **26,** 616–628
9. Gautam, R., Novak, E. K., Tan, J., Wakamatsu, K., Ito, S., and Swank, R. T. (2006) Interaction of Hermansky-Pudlak syndrome genes in the regulation of lysosome-related organelles. *Traffic* **7,** 779–792
10. Dell'Angelica, E. C. (2004) The building BLOC(k)s of lysosomes and related organelles. *Curr. Opin. Cell Biol.* **16,** 458–464
11. Dell'Angelica, E. C. (2009) AP-3-dependent trafficking and disease. The first decade. *Curr. Opin. Cell Biol.* **21,** 552–559
12. Bonifacino, J. S., and Traub, L. M. (2003) Signals for sorting of transmembrane proteins to endosomes and lysosomes. *Annu. Rev. Biochem.* **72,** 395–447
13. Peden, A. A., Oorschot, V., Hesser, B. A., Austin, C. D., Scheller, R. H., and Klumperman, J. (2004) Localization of the AP-3 adaptor complex defines a novel endosomal exit site for lysosomal membrane proteins. *J. Cell Biol.* **164,** 1065–1076
14. Raposo, G., and Marks, M. S. (2007) Melanosomes. Dark organelles enlighten endosomal membrane transport. *Nat. Rev. Mol. Cell Biol.* **8,** 786–797
15. Theos, A. C., Tenza, D., Martina, J. A., Hurbain, I., Peden, A. A., Sviderskaya, E. V., Stewart, A., Robinson, M. S., Bennett, D. C., Cutler, D. F., Bonifacino, J. S., Marks, M. S., and Raposo, G. (2005) Functions of adaptor protein (AP)-3 and AP-1 in tyrosinase sorting from endosomes to melanosomes. *Mol. Biol. Cell* **16,** 5356–5372
16. Hurbain, I., Geerts, W. J., Boudier, T., Marco, S., Verkleij, A. J., Marks, M. S., and Raposo, G. (2008) Electron tomography of early melanosomes. Implications for melanogenesis and the generation of fibrillar amyloid sheets. *Proc. Natl. Acad. Sci. U.S.A.* **105,** 19726–19731
17. Di Pietro, S. M., Falcón-Pérez, J. M., Tenza, D., Setty, S. R., Marks, M. S., Raposo, G., and Dell'Angelica, E. C. (2006) BLOC-1 interacts with BLOC-2 and the AP-3 complex to facilitate protein trafficking on endosomes. *Mol. Biol. Cell* **17,** 4027–4038

18. Setty, S. R., Tenza, D., Truschel, S. T., Chou, E., Sviderskaya, E. V., Theos, A. C., Lamoreux, M. L., Di Pietro, S. M., Starcevic, M., Bennett, D. C., Dell'Angelica, E. C., Raposo, G., and Marks, M. S. (2007) BLOC-1 is required for cargo-specific sorting from vacuolar early endosomes toward lysosome-related organelles. *Mol. Biol. Cell* **18,** 768–780
19. Salazar, G., Craige, B., Styers, M. L., Newell-Litwa, K. A., Doucette, M. M., Wainer, B. H., Falcon-Perez, J. M., Dell'Angelica, E. C., Peden, A. A., Werner, E., and Faundez, V. (2006) BLOC-1 complex deficiency alters the targeting of adaptor protein complex-3 cargoes. *Mol. Biol. Cell* **17,** 4014–4026
20. Delevoye, C., Hurbain, I., Tenza, D., Sibarita, J. B., Uzan-Gafsou, S., Ohno, H., Geerts, W. J., Verkleij, A. J., Salamero, J., Marks, M. S., and Raposo, G. (2009) AP-1 and KIF13A coordinate endosomal sorting and positioning during melanosome biogenesis. *J. Cell Biol.* **187,** 247–264
21. Marks, M. S., and Seabra, M. C. (2001) The melanosome: membrane dynamics in black and white. *Nat. Rev. Mol. Cell Biol.* **2,** 738–748
22. Rendu, F., and Brohard-Bohn, B. (2001) The platelet release reaction. Granules' constituents, secretion, and functions. *Platelets* **12,** 261–273
23. Zerial, M., and McBride, H. (2001) Rab proteins as membrane organizers. *Nat. Rev. Mol. Cell Biol.* **2,** 107–117
24. Hutagalung, A. H., and Novick, P. J. (2011) Role of Rab GTPases in membrane traffic and cell physiology. *Physiol. Rev.* **91,** 119–149
25. Loftus, S. K., Larson, D. M., Baxter, L. L., Antonellis, A., Chen, Y., Wu, X., Jiang, Y., Bittner, M., Hammer, J. A., 3rd, and Pavan, W. J. (2002) Mutation of melanosome protein RAB38 in chocolate mice. *Proc. Natl. Acad. Sci. U.S.A.* **99,** 4471–4476
26. Cohen-Solal, K. A., Sood, R., Marin, Y., Crespo-Carbone, S. M., Sinsimer, D., Martino, J. J., Robbins, C., Makalowska, I., Trent, J., and Chen, S. (2003) Identification and characterization of mouse Rab32 by mRNA and protein expression analysis. *Biochim. Biophys. Acta* **1651,** 68–75
27. Wasmeier, C., Romao, M., Plowright, L., Bennett, D. C., Raposo, G., and Seabra, M. C. (2006) Rab38 and Rab32 control post-Golgi trafficking of melanogenic enzymes. *J. Cell Biol.* **175,** 271–281
28. Brooks, B. P., Larson, D. M., Chan, C. C., Kjellstrom, S., Smith, R. S., Crawford, M. A., Lamoreux, L., Huizing, M., Hess, R., Jiao, X., Hejtmancik, J. F., Maminishkis, A., John, S. W., Bush, R., and Pavan, W. J. (2007) Analysis of ocular hypopigmentation in Rab38 cht/cht mice. *Invest. Ophthalmol. Vis. Sci.* **48,** 3905–3913
29. Osanai, K., Oikawa, R., Higuchi, J., Kobayashi, M., Tsuchihara, K., Iguchi, M., Jongsu, H., Toga, H., and Voelker, D. R. (2008) A mutation in Rab38 small GTPase causes abnormal lung surfactant homeostasis and aberrant alveolar structure in mice. *Am. J. Pathol.* **173,** 1265–1274
30. Oiso, N., Riddle, S. R., Serikawa, T., Kuramoto, T., and Spritz, R. A. (2004) The rat Ruby (R) locus is Rab38. Identical mutations in Fawn-hooded and Tester-Moriyama rats derived from an ancestral Long Evans rat substrain. *Mamm. Genome* **15,** 307–314
31. Ninkovic, I., White, J. G., Rangel-Filho, A., and Datta, Y. H. (2008) The role of Rab38 in platelet-dense granule defects. *J. Thromb. Haemost.* **6,** 2143–2151
32. Lopes, V. S., Wasmeier, C., Seabra, M. C., and Futter, C. E. (2007) Melanosome maturation defect in Rab38-deficient retinal pigment epithelium results in instability of immature melanosomes during transient melanogenesis. *Mol. Biol. Cell* **18,** 3914–3927
33. Marks, M. S. (2006) Darkness descends with two Rabs. *J. Cell Biol.* **175,** 199–200
34. Di Pietro, S. M., Falcón-Pérez, J. M., and Dell'Angelica, E. C. (2004) Characterization of BLOC-2, a complex containing the Hermansky-Pudlak syndrome proteins HPS3, HPS5, and HPS6. *Traffic* **5,** 276–283
35. Nazarian, R., Huizing, M., Helip-Wooley, A., Starcevic, M., Gahl, W. A., and Dell'Angelica, E. C. (2008) An immunoblotting assay to facilitate the molecular diagnosis of Hermansky-Pudlak syndrome. *Mol. Genet. Metab.* **93,** 134–144
36. Dell'Angelica, E. C., Aguilar, R. C., Wolins, N., Hazelwood, S., Gahl, W. A., and Bonifacino, J. S. (2000) Molecular characterization of the protein encoded by the Hermansky-Pudlak syndrome type 1 gene. *J. Biol. Chem.* **275,** 1300–1306
37. Kloer, D. P., Rojas, R., Ivan, V., Moriyama, K., van Vlijmen, T., Murthy, N., Ghirlando, R., van der Sluijs, P., Hurley, J. H., and Bonifacino, J. S. (2010) Assembly of the biogenesis of lysosome-related organelles complex-3 (BLOC-3) and its interaction with Rab9. *J. Biol. Chem.* **285,** 7794–7804
38. Nazarian, R., Starcevic, M., Spencer, M. J., and Dell'Angelica, E. C. (2006) Reinvestigation of the dysbindin subunit of BLOC-1 (biogenesis of lysosome-related organelles complex-1) as a dystrobrevin-binding protein. *Biochem. J.* **395,** 587–598
39. Ozeki, H., Ito, S., Wakamatsu, K., and Hirobe, T. (1995) Chemical characterization of hair melanins in various coat-color mutants of mice. *J. Invest. Dermatol.* **105,** 361–366
40. Dell'Angelica, E. C., Shotelersuk, V., Aguilar, R. C., Gahl, W. A., and Bonifacino, J. S. (1999) Altered trafficking of lysosomal proteins in Hermansky-Pudlak syndrome due to mutations in the β3A subunit of the AP-3 adaptor. *Mol. Cell* **3,** 11–21
41. Dell'Angelica, E. C., Ooi, C. E., and Bonifacino, J. S. (1997) β3A-adaptin, a subunit of the adaptor-like complex AP-3. *J. Biol. Chem.* **272,** 15078–15084
42. Kim, P. K., Mullen, R. T., Schumann, U., and Lippincott-Schwartz, J. (2006) The origin and maintenance of mammalian peroxisomes involves a *de novo* PEX16-dependent pathway from the ER. *J. Cell Biol.* **173,** 521–532
43. Valencia, J. C., Watabe, H., Chi, A., Rouzaud, F., Chen, K. G., Vieira, W. D., Takahashi, K., Yamaguchi, Y., Berens, W., Nagashima, K., Shabanowitz, J., Hunt, D. F., Appella, E., and Hearing, V. J. (2006) Sorting of Pmel17 to melanosomes through the plasma membrane by AP1 and AP2. Evidence for the polarized nature of melanocytes. *J. Cell Sci.* **119,** 1080–1091
44. Truschel, S. T., Simoes, S., Setty, S. R., Harper, D. C., Tenza, D., Thomas, P. C., Herman, K. E., Sackett, S. D., Cowan, D. C., Theos, A. C., Raposo, G., and Marks, M. S. (2009) ESCRT-I function is required for Tyrp1 transport from early endosomes to the melanosome limiting membrane. *Traffic* **10,** 1318–1336
45. Setty, S. R., Tenza, D., Sviderskaya, E. V., Bennett, D. C., Raposo, G., and Marks, M. S. (2008) Cell-specific ATP7A transport sustains copper-dependent tyrosinase activity in melanosomes. *Nature* **454,** 1142–1146
46. Tamura, K., Ohbayashi, N., Maruta, Y., Kanno, E., Itoh, T., and Fukuda, M. (2009) Varp is a novel Rab32/38-binding protein that regulates Tyrp1 trafficking in melanocytes. *Mol. Biol. Cell* **20,** 2900–2908
47. Helip-Wooley, A., Westbroek, W., Dorward, H. M., Koshoffer, A., Huizing, M., Boissy, R. E., and Gahl, W. A. (2007) Improper trafficking of melanocyte-specific proteins in Hermansky-Pudlak syndrome type-5. *J. Invest. Dermatol.* **127,** 1471–1478
48. Huizing, M., Sarangarajan, R., Strovel, E., Zhao, Y., Gahl, W. A., and Boissy, R. E. (2001) AP-3 mediates tyrosinase but not TRP-1 trafficking in human melanocytes. *Mol. Biol. Cell* **12,** 2075–2085
49. Tamura, K., Ohbayashi, N., Ishibashi, K., and Fukuda, M. (2011) Structure-function analysis of VPS9-ankyrin-repeat protein (Varp) in the trafficking of tyrosinase-related protein 1 in melanocytes. *J. Biol. Chem.* **286,** 7507–7521
50. Gautam, R., Chintala, S., Li, W., Zhang, Q., Tan, J., Novak, E. K., Di Pietro, S. M., Dell'Angelica, E. C., and Swank, R. T. (2004) The Hermansky-Pudlak syndrome 3 (cocoa) protein is a component of the biogenesis of lysosome-related organelles complex-2 (BLOC-2). *J. Biol. Chem.* **279,** 12935–12942
51. Huizing, M., Pederson, B., Hess, R. A., Griffin, A., Helip-Wooley, A., Westbroek, W., Dorward, H., O'Brien, K. J., Golas, G., Tsilou, E., White, J. G., and Gahl, W. A. (2009) Clinical and cellular characterization of Hermansky-Pudlak syndrome type 6. *J. Med. Genet.* **46,** 803–810
52. Kobayashi, T., and Hearing, V. J. (2007) Direct interaction of tyrosinase with Tyrp1 to form heterodimeric complexes *in vivo*. *J. Cell Sci.* **120,** 4261–4268
53. Bui, M., Gilady, S. Y., Fitzsimmons, R. E., Benson, M. D., Lynes, E. M., Gesson, K., Alto, N. M., Strack, S., Scott, J. D., and Simmen, T. (2010) Rab32 modulates apoptosis onset and mitochondria-associated membrane (MAM) properties. *J. Biol. Chem.* **285,** 31590–31602
54. Baust, T., Anitei, M., Czupalla, C., Parshyna, I., Bourel, L., Thiele, C., Krause, E., and Hoflack, B. (2008) Protein networks supporting AP-3 function in targeting lysosomal membrane proteins. *Mol. Biol. Cell* **19,** 1942–1951 10